Molecular and Cellular Endocrinology 523 (2021) 111139

Contents lists available at ScienceDirect

Molecular and Cellular Endocrinology

journal homepage: www.elsevier.com/locate/mce

Raman spectroscopy of follicular fluid and plasma with machine-learning algorithms for polycystic ovary syndrome screening

Xinyi Zhang [a,b], Bo Liang [c], Jun Zhang [d], Xinyao Hao [a,b], Xiaoyan Xu [a,b], Hsun-Ming Chang [e], Peter C.K. Leung [e,1,**], Jichun Tan [a,b,*,1]

[a] Center of Reproductive Medicine, Department of Obstetrics and Gynecology, Shengjing Hospital of China Medical University, Shenyang, Liaoning, China
[b] Key Laboratory of Reproductive Dysfunction Diseases and Fertility Remodeling of Liaoning Province, Shenyang, Liaoning, China
[c] State Key Laboratory of Microbial Metabolism, Joint International Research Laboratory of Metabolic and Developmental Sciences, School of Life Sciences and Biotechnology, Shanghai Jiao Tong University, Shanghai, China
[d] Basecare Medical Device Co., Jiangsu, China
[e] Department of Obstetrics and Gynaecology, BC Children's Hospital Research Institute, University of British Columbia, Vancouver, British Columbia, Canada

ARTICLE INFO

Keywords:
Polycystic ovary syndrome
Raman spectroscopy
Machine-learning algorithm
Follicular fluid
Screening

ABSTRACT

Polycystic ovary syndrome (PCOS) is the main cause of anovulatory infertility and affects women throughout their lives. The specific diagnostic method is still under investigation. In the present study, we aimed to identify the metabolic tracks of the follicular fluid and plasma samples from women with PCOS by performing Raman spectroscopy with principal component analysis and spectral classification models. Follicular fluid and plasma samples obtained from 50 healthy (non-PCOS) and 50 PCOS women were collected and measured by Raman spectroscopy. Multivariate statistical methods and different machine-learning algorithms based on the Raman spectra were established to analyze the results. The principal component analysis of the Raman spectra showed differences in the follicular fluid between the non-PCOS and PCOS groups. The stacking classification models based on the k-nearest-neighbor, random forests and extreme gradient boosting algorithms yielded a higher accuracy of 89.32% by using follicular fluid than the accuracy of 74.78% obtained with plasma samples in classifying the spectra from the two groups. In this regard, PCOS may lead to the changes of metabolic profiles that can be detected by Raman spectroscopy. As a novel, rapid and affordable method, Raman spectroscopy combined with advanced machine-learning algorithms have potential to analyze and characterize patients with PCOS.

1. Introduction

Polycystic ovary syndrome (PCOS) is the main cause of anovulatory infertility that affects 5–20% of women of reproductive age (Azziz et al., 2016). This endocrine disorder is a heterogeneous collection of signs and symptoms, including metabolic, reproductive and psychological implications (Teede et al., 2018). Moreover, women with PCOS are at higher risk for obstetrical complications, type II diabetes, cardiovascular disease, and endometrial cancer (Teede et al., 2011). Consequently, PCOS affects a woman's health over her life span.

Currently, there is no specific detection test to definitively diagnose PCOS. According to the Rotterdam criteria, diagnosis required the presence of at least two of the following three characteristics: ovulatory dysfunction, polycystic ovarian morphology on ultrasound and hyperandrogenism, with exclusion of other etiologies (Rotterdam, 2004). However, the effect of observer subjectivity in measurement, time-consuming methods, exclusive definition and delayed diagnosis are posing challenges to the diagnosis of PCOS (Balen et al., 2016; Gibson-Helm et al., 2017). Although a number of biomarker or genetic predisposition studies have been developed (Day et al., 2018; Sun et al.,

* Corresponding author. Center of Reproductive Medicine, Department of Obstetrics and Gynecology, Shengjing Hospital of China Medical University, Shenyang, Liaoning, China.
** Corresponding author. Department of Obstetrics and Gynecology, BC Children's Hospital Research Institute, University of British Columbia, Room 317, 950 west 28th Ave, Vancouver, British Columbia, V5Z 4H4, Canada.
E-mail addresses: peter.leung@ubc.ca (P.C.K. Leung), tjczjh@163.com (J. Tan).
[1] Peter C.K. Leung and Jichun Tan are co-corresponding authors.

https://doi.org/10.1016/j.mce.2020.111139
Received 31 October 2020; Received in revised form 4 December 2020; Accepted 18 December 2020
Available online 5 January 2021

2012; Zhao et al., 2019), the majority of these studies are limited by the clinical application due to diagnostic accuracy and costs. Therefore, an accurate, low-cost and reagent-less approach is required for performing the diagnosis and guiding the prevention and treatment of PCOS.

Abnormal folliculogenesis and impaired oocyte development are critical factors in the pathogenesis of PCOS, which have been linked with hyperandrogenism, insulin resistance, inflammation, and obesity (Ambekar et al., 2015; Diamanti-Kandarakis, 2008). Follicular fluid is a complex biological fluid, coordinating the somatic cell-oocyte interactions and serving as the specialized microenvironment for oocyte development and maturation (Dumesic et al., 2015). Follicular fluid levels of cytokines, growth factors, proteins, metabolites and noncoding RNAs have been reported to be associated with oocyte quality and pregnancy outcomes (Battaglia et al., 2017; Kollmann et al., 2017; O'Gorman et al., 2013). Therefore, studies on the specific components within the follicular fluid are vital to reveal potential biomarkers for oocyte development in women with PCOS treated with assisted reproductive technology.

Raman spectroscopy is a rapid and nondestructive method based on the inelastic scattering of light that provides the unique molecular fingerprints of relevant biological molecules. Application of Raman spectroscopy in combination with machine-learning algorithms has been developed as a noninvasive diagnostic approach for several diseases, such as endometriosis, Alzheimer's disease, hypertension, leukemia and cancers (Li et al., 2018a; Paraskevaidi et al., 2018b; Parlatan et al., 2019b). For example, serum samples obtained from patients with endometriosis were analyzed by Raman spectroscopy with PCA and classification algorithms (Parlatan et al., 2019a). Additionally, this technique has been implemented to diagnose plasma samples from patients with Alzheimer's disease and dementia (Paraskevaidi et al., 2018a). In the field of cancer research, improved classification algorithm has been established for breast cancer diagnosis based on the Raman spectra (Li et al., 2018b). Breast tissues of normal, fibrocystic change, fibroadenoma, and infiltrating carcinoma from patients were analyzed by Raman spectroscopy to diagnose the benign and malignant lesions (Haka et al., 2005b). Moreover, Raman spectra using blood samples has been reported to screen cervical and ovarian cancers (Lyng et al., 2015a; Owens et al., 2014a). This technique has brought new insights to reproductive medicine to reveal the chemical composition and constituents in very small sample volumes. The screening of breast, cervical and ovarian cancers by Raman spectroscopy have been reported (Haka et al., 2005a; Lyng et al., 2015b; Owens et al., 2014b). With technological advances, Raman spectroscopic analyses of oocytes, granulosa cells, embryos, seminal plasma, testicular cells and sperm have been increasingly studied (Mallidis et al., 2014; Notarstefano et al., 2019). The above studies suggested that Raman spectroscopy might be of potential value in the diagnosis of PCOS and in revealing metabolic profiles underlying this disease.

In the present study, we performed Raman spectroscopy combined with multivariate statistical methods to detect the metabolic tracks in follicular fluid and plasma samples from women with PCOS and healthy controls. We applied principal component analysis (PCA) to analyze data and further established spectral classification models based on machine-learning algorithms. We aimed at evaluating the diagnostic potential of Raman spectra-based classification models for women with PCOS.

2. Materials and methods

2.1. Participants

A total of 100 women (22–35 years of age) who underwent in vitro fertilization (IVF) in Shengjing Hospital of China Medical University were recruited to obtain informed consent, including 50 healthy (non-PCOS) women and 50 women with PCOS. The diagnosis of PCOS was based on the Rotterdam criteria of at least two of the following three features: oligo-ovulation and/or anovulation, polycystic ovary morphology on ultrasound and clinical or biochemical hyperandrogenism. Other etiologies such as congenital adrenal hyperplasia, androgen-secreting tumors, Cushing's syndrome, hyperprolactinemia, and cardiovascular disease were excluded. Patients who had been taking any kind of hormonal medication over the last three months were excluded from this study. Participants were instructed to wait for spontaneous menstruation without using prescribed progestins or oral contraceptives to control factors affecting the content of follicular fluid. The non-PCOS group included women with regular menstrual cycles and normal ovarian reserve who sought treatment for infertility due to a tubal or male factor. Clinical and biochemical characteristics of the participants are presented in Table 1.

2.2. Sample collection

Blood samples were collected on day 2 or day 3 of the menstrual cycle prior to the onset of controlled ovarian hyperstimulation. The blood samples were then centrifuged and stored at −80 °C for further analysis. Participants underwent controlled ovarian stimulation by either a gonadotropin-releasing hormone (GnRH) antagonist or a long GnRH agonist protocol, of which the former regimen was mainly administered in participants from PCOS and non-PCOS groups. Ovarian stimulation was performed by the combination of recombinant follicle-stimulating hormone (FSH) and human menopausal gonadotropin. Follicular development was monitored by ultrasonography, and blood hormone levels were measured. When there were two or more follicles that reached a diameter of ≥18 mm during ultrasound scanning, 250 μg of recombinant human chorionic gonadotropin (Ovidrel, Merck-Serono, Switzerland) was administered 35–37 h before oocyte retrieval. Follicular fluid samples were collected by transvaginal ultrasound-guided aspiration from size-matched follicles measured 20–22 mm after oocyte identification, without bloody contamination. All collected follicular fluid samples from each patient were pooled together and then centrifuged at 1000 g for 10 min to remove the cells and debris. The supernatant was stored at −80 °C for further use.

2.3. Spectra acquisition

Briefly, the follicular fluid and plasma samples were taken from −80 °C storage, thawed at room temperature and centrifuged prior to analysis. A total volume of 2 μL of the sample was drawn from the middle of the liquid and dropped onto a clean place on the surface of the sample test substrate without touching the substrate. Raman spectra were acquired from the Raman spectroscopy system (Basecare Raman 200) equipped with a 532 nm laser and a spectral resolution of 0.5 cm^{-1}. The spectral range was from 50 to 2000 cm^{-1}, and the accumulative times of a single point are 8 times. In general, 5 scattered points of each

Table 1
Description of the study participants.

	Non-PCOS	PCOS	*P*-value
Age (year)	30.24 ± 3.24	30.02 ± 3.47	NS
BMI (kg/m^2)	22.33 ± 3.70	26.47 ± 3.76	$P < 0.001$
Total testosterone (ng/ml)	0.47 ± 0.14	0.75 ± 0.24	$P < 0.001$
FSH (IU/l)	7.11 ± 2.05	7.11 ± 2.10	NS
LH (IU/l)	5.66 ± 3.01	10.42 ± 4.79	$P < 0.001$
Estradiol (pg/ml)	46.95 ± 16.62	50.90 ± 14.56	NS
Fasting glucose (mmol/l)	5.16 ± 0.65	5.22 ± 0.47	NS
Fasting insulin (mU/l)	10.69 ± 4.87	16.02 ± 8.15	$P < 0.001$
Total cholesterol (mmol/l)	4.26 ± 0.77	4.66 ± 0.80	$P < 0.05$
LDL-C (mmol/l)	2.51 ± 0.62	2.90 ± 0.63	$P < 0.01$
HDL-C (mmol/l)	1.33 ± 0.35	1.13 ± 0.30	$P < 0.01$
Triglycerides (mmol/l)	0.98 ± 0.62	1.90 ± 1.44	$P < 0.001$

Note: BMI, body mass index; FSH, follicle-stimulating hormone; LH, luteinizing hormone; LDL-C, low-density lipoprotein cholesterol; HDL-C, high-density lipoprotein cholesterol; NS, not significant. Data are presented as mean ± SD.

sample were selected to reduce the bias in testing, based on the preliminary experiment results.

2.4. Spectral data processing and analysis

It is well-known that the characteristic peaks of Raman spectra contain abundant material structure information, composition and content. In this regard, spectral analysis must rely on machine-learning data sets and bioinformatics methods to carry out full-spectrum pattern recognition analysis based on the complex multivariate data of samples. The raw Raman spectra obtained in this study were preprocessed by an inhouse program on Python 3.5, cropped to the region of 600 to 1800 cm^{-1}, and pre-processed by the steps of wavelet denoising and vector normalization. We used internal scripts for multivariate analysis, statistics and visualization in the R environment. Raman data sets and R code have been displayed at: https://1drv.ms/u/s!AueePmluaEFYg_VJW_zMi7JkWVW6Ig?e=Ngiwv9. The unsupervised PCA method was used to analyze the Raman data, which can extract key features, reduce the high dimensionality of the data and determine principal components (PCs). In general, the first 3 PCs accounted for more than 90% of the variance of the selected spectral regions. The loading plots derived by PCA were used as the distribution spectrum of the most important variables (Raman shift bands), which contributed to the structure of the data matrix and could be associated with the molecular bonds corresponding to the specific wavenumber of the Raman shift.

2.5. Machine-learning classification

Non-PCOS women and PCOS patients were classified by machine-learning models based on the original Raman spectra. There were two independent spectral data sets, one from the follicular fluid samples and the other from the plasma samples. Each spectral data set was divided into a training set and testing set at a ratio of 4:1. We used the training set to train the classification model and the testing set to evaluate model performance. As previously described, three machine-learning algorithms, including k-nearest neighbors (kNN), random forests (RF) and extreme gradient boosting (XGB), were used separately and then stacked together to construct another machine-learning model (Liang et al., 2019). According to the results, performance measurements, including the sensitivity, specificity and accuracy of the classification models were calculated, which can indicate the classification performance for predicting samples. The definitions are displayed below, of which TP refers to the number of true positives, FP refers to the number of false positives, TN refers to the number of true negatives and FN refers to the number of false negatives.

$$\text{Sensitivity} = TP / (TP + FN)$$

$$\text{Specificity} = TN / (TN + FP)$$

$$\text{Accuracy} = (TP + TN) / (TP + TN + FP + FN)$$

3. Results and discussion

3.1. Biomolecular analysis of follicular fluid samples based on Raman spectroscopy

Raman spectroscopy can indicate the metabolic profiles of biological molecules in different organisms, infer the physiological changes of the body and thus diagnose diseases. In this study, we obtained data sets from Raman spectra of 50 women without PCOS and 50 women with PCOS by analyzing follicular fluid samples. The fingerprint region in the range of 600 cm^{-1} to 1800 cm^{-1} was calculated and is displayed in Fig. 1, for which the relative intensities of the spectra were manually separated for visual presentation. There was no significant difference in the mean spectra of the non-PCOS and PCOS groups.

The PCA statistical method was then utilized to reduce the number of variables and extract key information from the original spectrum. In this study, three PCs with the highest contribution rates were selected for analyses. The PCA score plots of dimensions 1 vs. 2 and dimensions 1 vs. 3 illustrated distinct (despite some overlaps) segregations between the non-PCOS and PCOS groups (Fig. 2). The quantification results in the boxplots show significant differences in all three Raman spaces between the two groups ($P < 0.001$) of follicular fluid samples (Fig. 3A, C and 3E). Similarly, the quantification results in the boxplots show significant differences in all three Raman spaces between the two groups ($P < 0.001$) of their plasma samples (Supplementary Fig. 1A, 1B and 1C). Several peaks labeled on the loading graph revealed shifts and variations. The Raman loading plots along the three dimensions of PCA indicated that the differences between the non-PCOS and PCOS groups may be represented by Raman shifts at 1130–1150 cm^{-1} and 1480–1550 cm^{-1} (Fig. 3B, D and 3F). Changes in the characteristic peaks of Raman spectra provide a basis for molecular fingerprints of disease.

3.2. Biomolecular analysis of plasma samples based on Raman spectroscopy

The diagnostic method of blood testing is easy and noninvasive for

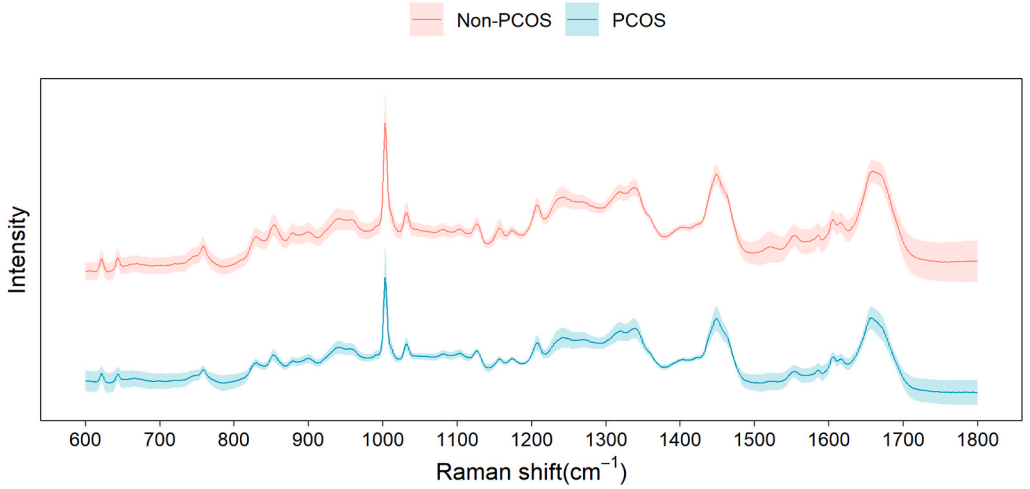

Fig. 1. Normalized Raman spectra of follicular fluid samples from the non-PCOS and PCOS groups. The standard deviations of each group are represented as shaded areas.

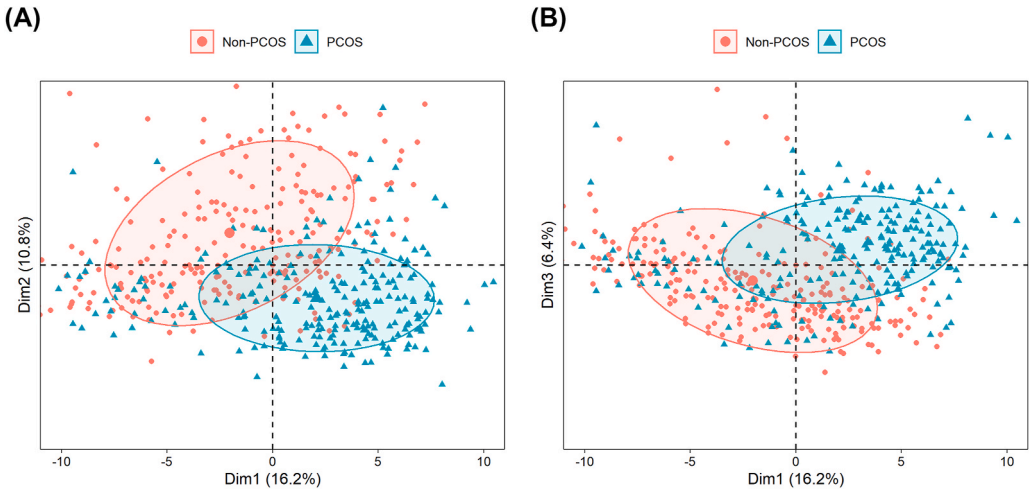

Fig. 2. Principal component analysis (PCA) plot of Raman spectra from follicular fluid samples. (A) PC1 vs. PC2 and (B) PC1 vs. PC3 score plots show clustering of non-PCOS and PCOS women.

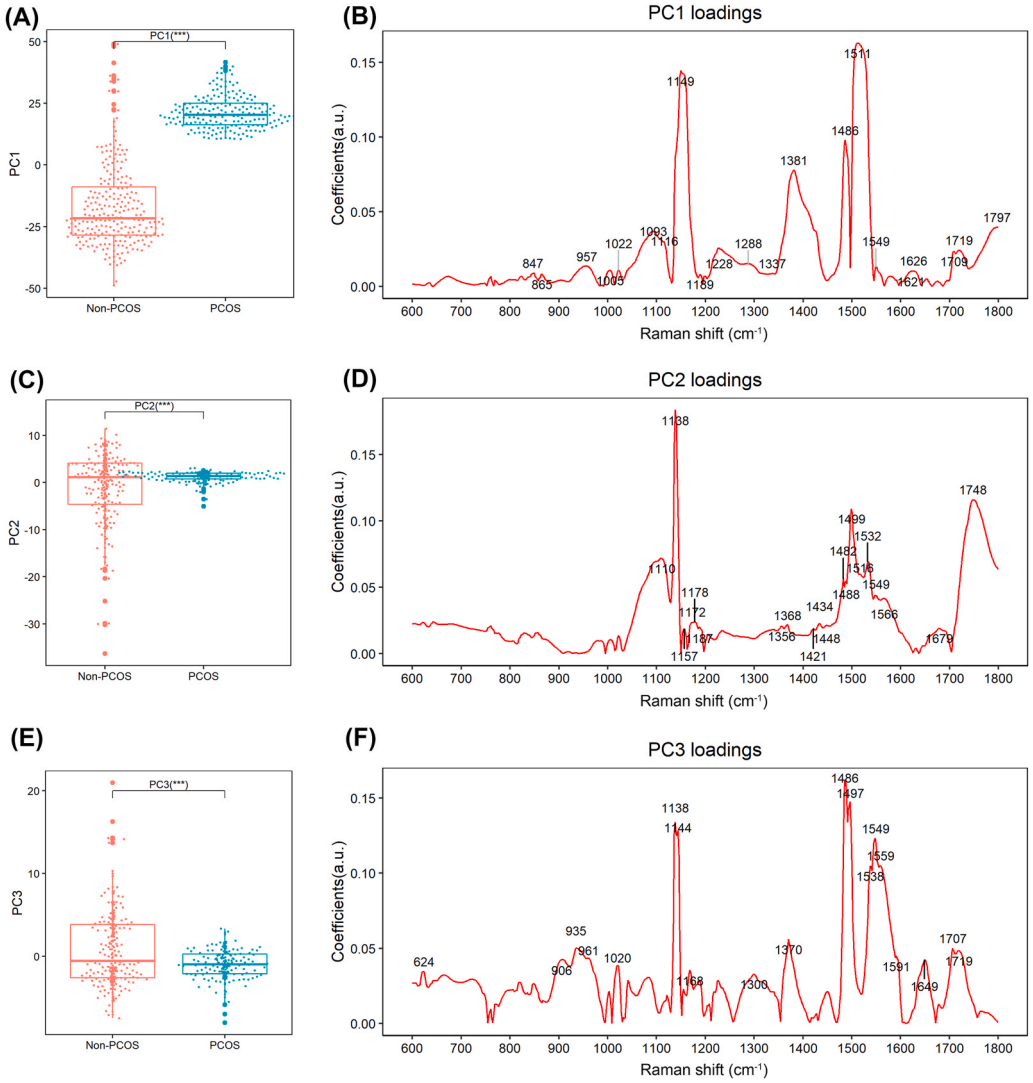

Fig. 3. Boxplots of Raman band integration of non-PCOS and PCOS follicular fluid samples, showing significant differences between the two groups. (A) PC1, (C) PC2, and (E) PC3; PC means were compared by the Welch 2-sample *t*-test for unequal variances: ***$P < 0.001$. Raman loading plots of the contributions for (B) PC1, (D) PC2, and (F) PC3 are presented.

many medical diseases and aid in decision-making for treatment. In our study, the plasma Raman spectra of the included non-PCOS and PCOS women were acquired and analyzed. Similarly, the average Raman spectra of the plasma samples from non-PCOS and PCOS women were calculated in the range of 600 cm^{-1} to 1800 cm^{-1}, as displayed in Fig. 4A. There was no significant difference in the mean spectra of the two groups, and the fingerprint regions of the collected Raman spectra were analyzed by PCA. In the PCA scoring plots for dimensions 1 vs. 2 and dimensions 1 vs. 3 based on data from the plasma samples, the overlap between the non-PCOS and PCOS groups was obvious compared with the results for the follicular fluid samples (Fig. 4B and C).

3.3. Machine-learning models based on Raman spectra for classifying non-PCOS and PCOS samples

After using PCA to extract information variables derived from the Raman spectra, we further examined the performance of the machine-learning algorithms on the classification of the Raman spectral data by using kNN, RF, and XGB models. To achieve more accurate results, these three models were further combined to train a stacking classification model. Generally, the performance of the three models and the stacking model were evaluated in terms of sensitivity, specificity, and accuracy. The results are presented in Table 2 and Table 3. As a single model, the application of KNN to the spectral data outperformed the other models in terms of sensitivity, specificity and accuracy in classifying PCOS and non-PCOS follicular fluid samples. There was a higher classification

Table 2
Performance evaluation of the kNN, RF, XGB and stacking classification models based on the Raman spectra from follicular fluid samples.

	Model	Sensitivity	Specificity	Accuracy
Follicular fluid	kNN	87.27%	89.80%	88.46%
	RF	82.76%	81.63%	82.24%
	XGB	84.21%	83.67%	83.96%
	Stacking	88.89%	89.80%	89.32%

Note: kNN, k-nearest neighbors; RF, random forests; XGB, extreme gradient boosting. The stacking analysis is based on a first layer based on kNN, RF and XGB and a second layer based on XGB. All results are presented in percentages.

Table 3
Performance evaluation of the kNN, RF, XGB and stacking classification models based on the Raman spectra from plasma samples.

	Model	Sensitivity	Specificity	Accuracy
Plasma	kNN	70.59%	74.00%	72.03%
	RF	68.57%	66.00%	67.50%
	XGB	72.73%	72.00%	72.41%
	Stacking	73.85%	76.00%	74.78%

Note: kNN, k-nearest neighbors; RF, random forests; XGB, extreme gradient boosting. The stacking analysis is based on a first layer based on kNN, RF and XGB and a second layer based on XGB. All results are presented in percentages.

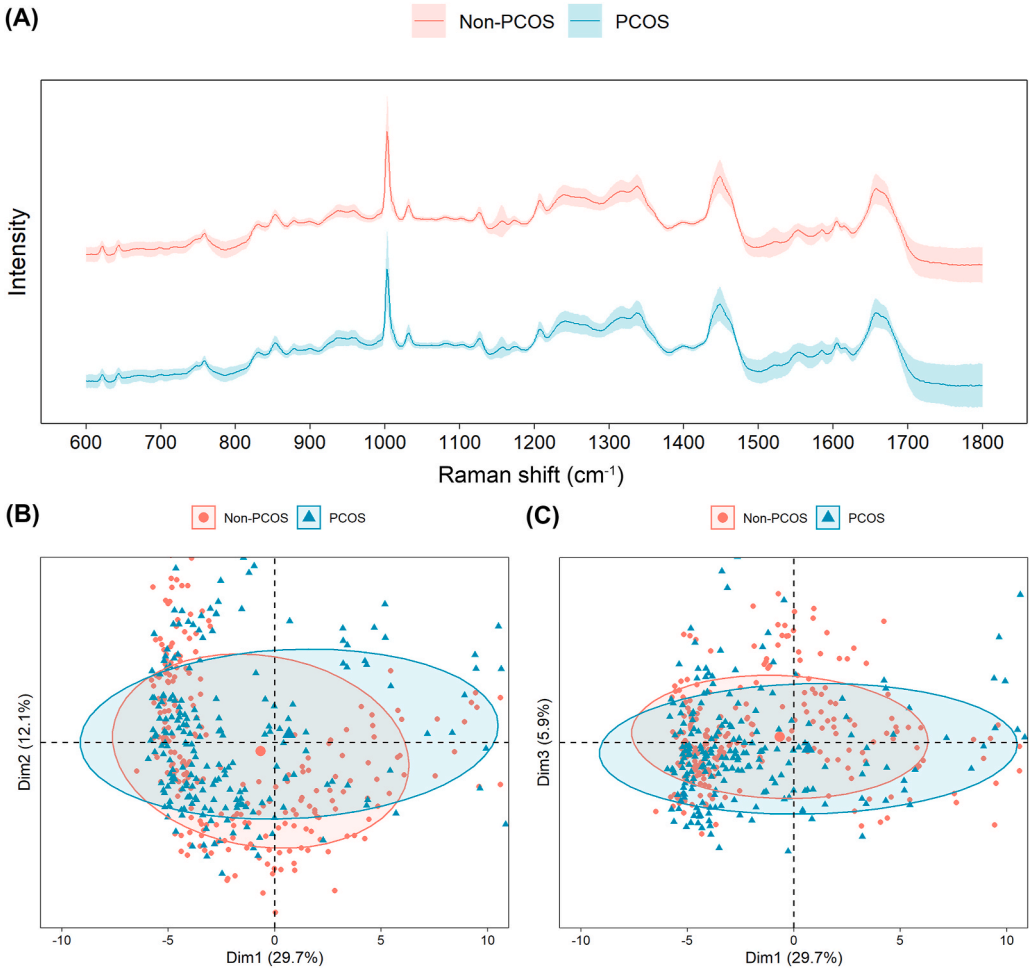

Fig. 4. (A) Normalized Raman spectra of plasma samples from the non-PCOS and PCOS groups. The standard deviations of each group are represented as shaded areas. Principal component analysis (PCA) plot of the Raman spectra of plasma samples. (B) PC1 vs. PC2 and (C) PC1 vs. PC3 score plots show the obvious overlap between non-PCOS and PCOS women.

model accuracy of 88.46% for the KNN model, compared with 82.24% for the RF model and 83.96% for the XGB model. In addition, the stacking model exhibited superior performance in terms of the classification model accuracy of 89.32%. However, the overall accuracy of the kNN, RF, XGB and stacking classification models in assessing performance did not exceed 80% when using plasma samples. The receiver operating characteristics (ROC) curves were further performed to investigate the classifier performance. In particular, the Stacking algorithm reached the highest AUC of 0.920 based on the analysis of follicular fluid samples (Supplementary Figure 2).

Due to the common metabolic disorders and long-term complications in PCOS patients, the number of studies of metabolic profiles characterizing different phenotypes, revealing pathways and identifying biochemical markers of PCOS are increasing (Buszewska-Forajta et al., 2019; Chang et al., 2017; Zhao et al., 2012). Raman spectroscopy is a label-free method used to detect metabolic profiles of samples. To the best of our knowledge, the research on Raman spectroscopy in diagnosing PCOS is still limited. One study has reported the use of the surface-enhanced Raman scattering (SERS) method to detect PCOS, demonstrating that the SERS technique in conjunction with PCA could classify between PCOS and non-PCOS women by using follicular fluid samples (Momenpour et al., 2018). In our study, we further analyzed both follicular fluid and plasma samples for women with PCOS with the use of Raman spectroscopy and reported the sensitivity, specificity and accuracy of machine-learning algorithms. The results were obtained rapidly with very small sample volumes and easy procedures, suggesting that the Raman spectra-based technique may be useful in the diagnosis of PCOS. Because of the heterogeneity of women with PCOS, subgroup analyses of larger participants are needed to validate the application of Raman spectroscopy in the diagnosis of PCOS.

This is a preliminary study investigating the application of Raman spectroscopy combined with machine-learning algorithms in PCOS. We analyzed the spectra data of both follicular fluid and plasma samples, in an attempt to reveal the intra-follicular and circulating metabolic changes of PCOS. Our results indicated that the metabolic differences exist, providing more evidence on the abnormal follicular development in patients with PCOS. One of the limitations of this study is that follicular fluid samples have been obtained by controlled ovarian hyperstimulation, instead of the non-controlled conditions. Additionally, analysis of the follicular fluid has limited practice in clinical diagnosis due to the invasive procedure, especially for adolescents and patients without fertility requirement. Moreover, caution should be taken when expanding our results to PCOS patients with atypical characteristics.

As a main cause of anovulatory infertility, PCOS patients who are receiving IVF are at a high risk of developing follicular dysplasia. The process of Raman analysis could be achieved rapidly with a small sample volume and an easy procedure. In addition, the model may be improved by including a larger sample size with more clinical parameters. Thus, we speculate that Raman spectroscopy analysis of follicular fluid with advanced machine-learning models have prospective application in predicting oocyte quality during the assisted reproductive technology, which may improve the clinical pregnancy rate in infertile PCOS patients.

Developing a rapid method for PCOS is challenging. Blood sample testing has been widely applied in the clinical diagnosis. We initially aimed to establish a diagnostic model based on the results of plasma Raman spectra. However, the performance of the current classification model was not satisfactory. We speculate that the results may be affected by multiple factors, including the sampling method, testing, and criteria of inclusion. Moreover, circulating hormone levels and metabolites could affect the results of Raman spectra analysis. Therefore, further studies with a larger sample size and subgroup analysis are needed.

4. Conclusion

The application of Raman spectroscopy showed significant differences between the non-PCOS and PCOS groups. Machine-learning models based on Raman spectra could classify the two groups with higher accuracy by using follicular fluid rather than plasma samples. Differences in the spectral bands of the Raman spectra possibly indicate molecular changes and biomarkers of PCOS. In summary, Raman spectroscopy revealed the changes of metabolic profiles in PCOS patients. Machine-learning models could classify the spectra from non-PCOS and PCOS groups with a higher accuracy based on the follicular fluid. As a novel, rapid and affordable method, Raman spectroscopy combined with advanced machine-learning algorithms may be a useful tool to analyze and characterize patients with PCOS.

Disclosure summary

The authors have nothing to disclose.

Financial support

The project was financed by National Key Research and Development Program (2018YFC1002105). This project was also supported by the CIHR Foundation Scheme Grant #143317 to P.C.K.L.

CRediT authorship contribution statement

Xinyi Zhang: conceived and designed research, performed experiments, analyzed data, interpreted results of experiments, drafted manuscript. **Bo Liang:** performed experiments. **Jun Zhang:** analyzed data. **Xinyao Hao:** interpreted results of experiments. **Xiaoyan Xu:** interpreted results of experiment. **Hsun-Ming Chang:** drafted manuscript. **Peter C.K. Leung:** conceived and designed research, edited and revised manuscript. **Jichun Tan:** conceived and designed research, edited and revised manuscript, Xinyi Zhang, Bo Liang, Jun Zhang, Xinyao Hao, Xiaoyan Xu, Hsun-Ming Chang, Peter C.K. Leung and Jichun Tan approved final version of manuscript.

Declaration of competing interest

All authors have no conflict of interest to declare.

Acknowledgments

We would like to thank technical support from Basecare Medical Device Company.

Appendix A. Supplementary data

Supplementary data to this article can be found online at https://doi.org/10.1016/j.mce.2020.111139.

References

Ambekar, A.S., Kelkar, D.S., Pinto, S.M., Sharma, R., Hinduja, I., Zaveri, K., Pandey, A., Prasad, T.S.K., Gowda, H., Mukherjee, S., 2015. Proteomics of follicular fluid from women with polycystic ovary syndrome suggests molecular defects in follicular development. J. Clin. Endocrinol. Metab. 100, 744–753.

Azziz, R., Carmina, E., Chen, Z., Dunaif, A., Laven, J.S.E., Legro, R.S., Lizneva, D., Natterson-Horowtiz, B., Teede, H.J., Yildiz, B.O., 2016. Polycystic ovary syndrome. Nat Rev Dis Prim 2, 16057-16057.

Balen, A.H., Morley, L.C., Misso, M., Franks, S., Legro, R.S., Wijeyaratne, C.N., Stener-Victorin, E., Fauser, B.C.J.M., Norman, R.J., Teede, H., 2016. The management of anovulatory infertility in women with polycystic ovary syndrome: an analysis of the evidence to support the development of global WHO guidance. Hum. Reprod. Update 22, 687–708.

Battaglia, R., Vento, M.E., Borzì, P., Ragusa, M., Barbagallo, D., Arena, D., Purrello, M., Di Pietro, C., 2017. Non-coding RNAs in the ovarian follicle. Front. Genet. 8, 57-57.

Buszewska-Forajta, M., Rachoń, D., Stefaniak, A., Wawrzyniak, R., Konieczna, A., Kowalewska, A., Markuszewski, M.J., 2019. Identification of the metabolic fingerprints in women with polycystic ovary syndrome using the multiplatform metabolomics technique. J. Steroid Biochem. Mol. Biol. 186, 176–184.

Chang, A.Y., Lalia, A.Z., Jenkins, G.D., Dutta, T., Carter, R.E., Singh, R.J., Nair, K.S., 2017. Combining a nontargeted and targeted metabolomics approach to identify metabolic pathways significantly altered in polycystic ovary syndrome. Metabolism 71, 52–63.

Day, F., Karaderi, T., Jones, M.R., Meun, C., He, C., Drong, A., Kraft, P., Lin, N., Huang, H., Broer, L., et al., 2018. Large-scale genome-wide meta-analysis of polycystic ovary syndrome suggests shared genetic architecture for different diagnosis criteria. PLoS Genet. 14 e1007813-e1007813.

Diamanti-Kandarakis, E., 2008. Polycystic ovarian syndrome: pathophysiology, molecular aspects and clinical implications. Expet Rev. Mol. Med. 10 e3-e3.

Dumesic, D.A., Meldrum, D.R., Katz-Jaffe, M.G., Krisher, R.L., Schoolcraft, W.B., 2015. Oocyte environment: follicular fluid and cumulus cells are critical for oocyte health. Fertil. Steril. 103, 303–316.

Gibson-Helm, M., Teede, H., Dunaif, A., Dokras, A., 2017. Delayed diagnosis and a lack of information associated with dissatisfaction in women with polycystic ovary syndrome. J. Clin. Endocrinol. Metab. 102, 604–612.

Haka, A.S., Shafer-Peltier, K.E., Fitzmaurice, M., Crowe, J., Dasari, R.R., Feld, M.S., 2005a. Diagnosing breast cancer by using Raman spectroscopy. Proc. Natl. Acad. Sci. U. S. A. 102, 12371–12376.

Haka, A.S., Shafer-Peltier, K.E., Fitzmaurice, M., Crowe, J., Dasari, R.R., Feld, M.S., 2005b. Diagnosing breast cancer by using Raman spectroscopy. Proc. Natl. Acad. Sci. U. S. A. 102, 12371–12376.

Kollmann, Z., Schneider, S., Fux, M., Bersinger, N.A., von Wolff, M., 2017. Gonadotrophin stimulation in IVF alters the immune cell profile in follicular fluid and the cytokine concentrations in follicular fluid and serum. Hum. Reprod. 32, 820–831.

Li, Q., Li, W., Zhang, J., Xu, Z., 2018a. An improved k-nearest neighbour method to diagnose breast cancer. Analyst 143, 2807–2811.

Li, Q., Li, W., Zhang, J., Xu, Z., 2018b. An improved k-nearest neighbour method to diagnose breast cancer. Analyst 143, 2807–2811.

Liang, B., Gao, Y., Xu, J., Song, Y., Xuan, L., Shi, T., Wang, N., Hou, Z., Zhao, Y.-L., Huang, W.E., et al., 2019. Raman profiling of embryo culture medium to identify aneuploid and euploid embryos. Fertil. Steril. 111, 753–762 e751.

Lyng, F.M., Traynor, D., Ramos, I.R., Bonnier, F., Byrne, H.J., 2015a. Raman spectroscopy for screening and diagnosis of cervical cancer. Anal. Bioanal. Chem. 407, 8279–8289.

Lyng, F.M., Traynor, D., Ramos, I.R.M., Bonnier, F., Byrne, H.J., 2015b. Raman spectroscopy for screening and diagnosis of cervical cancer. Anal. Bioanal. Chem. 407, 8279–8289.

Mallidis, C., Sanchez, V., Wistuba, J., Wuebbeling, F., Burger, M., Fallnich, C., Schlatt, S., 2014. Raman microspectroscopy: shining a new light on reproductive medicine. Hum. Reprod. Update 20, 403–414.

Momenpour, A., Lima, P.D.A., Chen, Y.A., Tzeng, C.R., Tsang, B.K., Anis, H., 2018. Surface-enhanced Raman scattering for the detection of polycystic ovary syndrome. Biomed. Optic Express 9, 801–817.

Notarstefano, V., Gioacchini, G., Byrne, H.J., Zacà, C., Sereni, E., Vaccari, L., Borini, A., Carnevali, O., Giorgini, E., 2019. Vibrational characterization of granulosa cells from patients affected by unilateral ovarian endometriosis: new insights from infrared and Raman microspectroscopy. Spectrochim. Acta Mol. Biomol. Spectrosc. 212, 206–214.

O'Gorman, A., Wallace, M., Cottell, E., Gibney, M.J., McAuliffe, F.M., Wingfield, M., Brennan, L., 2013. Metabolic profiling of human follicular fluid identifies potential biomarkers of oocyte developmental competence. Reproduction 146, 389–395.

Owens, G.L., Gajjar, K., Trevisan, J., Fogarty, S.W., Taylor, S.E., Da Gama-Rose, B., Martin-Hirsch, P.L., Martin, F.L., 2014a. Vibrational biospectroscopy coupled with multivariate analysis extracts potentially diagnostic features in blood plasma/serum of ovarian cancer patients. J. Biophot. 7, 200–209.

Owens, G.L., Gajjar, K., Trevisan, J., Fogarty, S.W., Taylor, S.E., Da Gama-Rose, B., Martin-Hirsch, P.L., Martin, F.L., 2014b. Vibrational biospectroscopy coupled with multivariate analysis extracts potentially diagnostic features in blood plasma/serum of ovarian cancer patients. J. Biophot. 7, 200–209.

Paraskevaidi, M., Morais, C.L.M., Halliwell, D.E., Mann, D.M.A., Allsop, D., Martin-Hirsch, P.L., Martin, F.L., 2018a. Raman spectroscopy to diagnose Alzheimer's disease and dementia with lewy bodies in blood. ACS Chem. Neurosci. 9, 2786–2794.

Paraskevaidi, M., Morais, C.L.M., Halliwell, D.E., Mann, D.M.A., Allsop, D., Martin-Hirsch, P.L., Martin, F.L., 2018b. Raman spectroscopy to diagnose Alzheimer's disease and dementia with lewy bodies in blood. ACS Chem. Neurosci. 9, 2786–2794.

Parlatan, U., Inanc, M.T., Ozgor, B.Y., Oral, E., Bastu, E., Unlu, M.B., Basar, G., 2019a. Raman spectroscopy as a non-invasive diagnostic technique for endometriosis. Sci. Rep. 9, 19795.

Parlatan, U., Inanc, M.T., Ozgor, B.Y., Oral, E., Bastu, E., Unlu, M.B., Basar, G., 2019b. Raman spectroscopy as a non-invasive diagnostic technique for endometriosis. Sci. Rep. 9, 19795-19795.

Sun, L., Hu, W., Liu, Q., Hao, Q., Sun, B., Zhang, Q., Mao, S., Qiao, J., Yan, X., 2012. Metabonomics reveals plasma metabolic changes and inflammatory marker in polycystic ovary syndrome patients. J. Proteome Res. 11, 2937–2946.

Teede, H.J., Misso, M.L., Deeks, A.A., Moran, L.J., Stuckey, B.G.A., Wong, J.L.A., Norman, R.J., Costello, M.F., Guideline Development, G., 2011. Assessment and management of polycystic ovary syndrome: summary of an evidence-based guideline. Med. J. Aust. 195, S65–S112.

Teede, H.J., Misso, M.L., Boyle, J.A., Garad, R.M., McAllister, V., Downes, L., Gibson, M., Hart, R.J., Rombauts, L., Moran, L., et al., 2018. Translation and implementation of the Australian-led PCOS guideline: clinical summary and translation resources from the international evidence-based guideline for the assessment and management of polycystic ovary syndrome. Med. J. Aust. 209, S3–S8.

Zhao, Y., Fu, L., Li, R., Wang, L.N., Yang, Y., Liu, N.N., Zhang, C.M., Wang, Y., Liu, P., Tu, B.B., et al., 2012. Metabolic profiles characterizing different phenotypes of polycystic ovary syndrome: plasma metabolomics analysis. BMC Med. 10, 153.

Zhao, Y., Zhao, Y., Wang, C., Liang, Z., Liu, X., 2019. Diagnostic value OF anti-müllerian hormone as a biomarker for polycystic ovary syndrome: a meta-analysis update. Endocr. Pract. 25, 1056–1066.